Supporting Information

Mechanistic Study of Asymmetric Oxidative Biaryl Coupling: Evidence for Self-Processing of the Copper Catalyst to Achieve Control of Oxidase vs. Oxygenase Activity

J. Brian Hewgley, Shannon S. Stahl, and Marisa C. Kozlowski

Department of Chemistry, Roy and Diana Vagelos Laboratories, University of Pennsylvania, Philadelphia, Pennsylvania 19104-6323, USA, and Department of Chemistry, University of Wisconsin-Madison, 1101 University Avenue, Madison, Wisconsin 53706

General Considerations	S2
Calibration Procedure	S2
Single Turnover Experiment with **1**	S3
Preparation of **4**	S4
Oxidation of **4** in the Presence of Unreactive Phenol **5**	S5
Discovery of the Initial Product Burst with **1**	S6
Correlation of O_2 Uptake to Product Formation and Substrate Consumption	S6
Stoichiometry of Dioxygen Uptake vs. Consumption of **2**	S7
General Procedure for Gas-Uptake Rate Measurements	S8
Steady-State Rate Extrapolation	S9
Steady-State Rate Dependence on [**4**]	S10
Steady-State Rate Dependence on pO_2	S11
Steady-State Rate Dependence on [**2**]	S12
Isolation of ortho-Quinone Species	S13
X-Ray Structure Determination of **4**	S15
X-Ray Structure Determination of **9**	S20
References	S27

General Considerations. Copper(I) iodide (Strem) was used without further purification. Oxygen (BOC), CH_3CN (Aldrich), and CH_2Cl_2 (Aldrich) were used without purification. 4-Biphenyl-phenyl ether (Pfaltz and Bauer) was recrystallized prior to use from ethanol (Fisher). When necessary, solvents and reagents were dried prior to use. CH_2Cl_2 was deoxygenated by purging with N_2 and then dried by passing through activated alumina. CH_3CN was distilled from CaH_2. 1,5-Diaza-*cis*-decalin was prepared as previously described.[1]

Analytical thin layer chromatography (TLC) was performed on EM Reagents 0.25 mm silica-gel 60-F plates. Visualization was accomplished with UV light. Chromatography on silica gel was performed using a forced flow of the indicated solvent system on EM Reagents Silica Gel 60 (230-400 mesh).[2] GC analysis for reactions was conducted with either a Shimadzu GC-17A gas chromatograph or an Agilent 6850 gas chromatograph with an HP-1 column (Agilent): length = 30 m, ID = 0.32 mm, film = 0.25 mm; flow = 2 mL/min, 165 °C to 290 °C. HPLC analysis of reactions was conducted on an Agilent 1100 liquid chromatograph with a UV detector (254 nm), a Chiralpak AD column (Chiral Technologies Inc., 0.46 cm, 25 cm), and hexanes (Fisher) and *i*-PrOH (Fisher) as the mobile phase. ^{1}H NMR spectra were recorded on a Bruker AM-500 (500 MHz) spectrometer. Chemical shifts are reported in ppm from tetramethylsilane (0 ppm) or from the solvent resonance ($CDCl_3$ 7.26 ppm, CD_3CN 1.94 ppm). Data are reported as follows: chemical shift, multiplicity (s = singlet, d = doublet, t = triplet, q = quartet, br = broad, m = multiplet), coupling constants, number of protons, and assignment. Proton decoupled ^{13}C NMR spectra were recorded on a Bruker AM-500 (500 MHz) spectrometer. Chemical shifts are reported in ppm from the solvent resonance ($CDCl_3$ 77.23 ppm, CD_3CN 118.3 ppm). Dioxygen uptake kinetics were performed using a computer-interfaced gas-uptake apparatus with a calibrated volume and a pressure transducer designed to measure the gas pressure within a sealed reaction vessel.[3] Data were acquired using custom software written within LabVIEW (National Instruments).

Calibration Procedure. Calibration curves for each analyte and 4-biphenyl phenyl ether (BPPE) were obtained by subjecting a series of analyte/BPPE mixtures with known molar concentration ratios (determined gravimetrically or by ^{1}H NMR) to GC or HPLC analysis. The area ratios from GC or HPLC were plotted against the molar concentration (see eq S1) ratios and the slope as determined by least squares was taken as the correction factor (*cf)* (see eq S2). For any given sample, then, the analyte concentration could be determined provided that the BPPE concentration was known (eq S3).

$$\frac{A_{analyte}}{A_{STD}} = \frac{\varepsilon_{analyte}}{\varepsilon_{STD}} \times \frac{[analyte]}{[STD]} \qquad (S1)$$

$A_{analyte}$ = analyte area from HPLC or GC trace, A_{STD} = BPPE area from HPLC or GC trace

$\varepsilon_{analyte}$ = analyte molar absorptivity (M^{-1}), ε_{STD} = BPPE molar absorptivity (M^{-1})

[analyte] = analyte concentration (M), [STD] = BPPE concentration (M)

$$\frac{\varepsilon_{analyte}}{\varepsilon_{STD}} = slope = cf \qquad (S2)$$

observable

$$\frac{A_{analyte} / A_{STD}}{cf} \times [STD] = [analyte] \qquad (S3)$$

known concentration of BPPE in sample

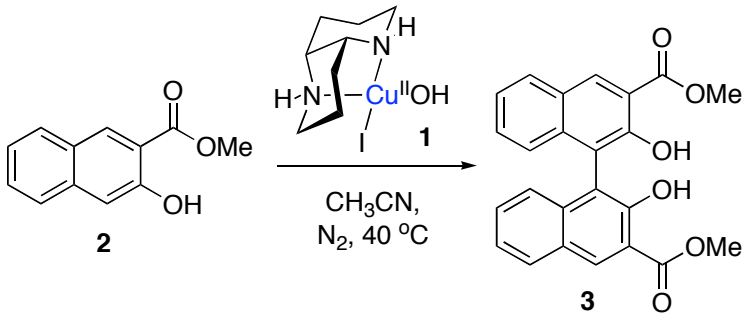

Single Turnover Experiment with 1. A Schlenk tube charged with **2** (85.2 mg, 0.42 mmol) and **1** (29.4 mg, 0.085 mmol) was taken into an inert atmosphere glovebox. The tube was then charged with degassed CH_3CN (5.2 mL), sealed with a Teflon® screw cap, removed from the glovebox, and sonicated to afford a homogenous solution. The resulting solution was heated at 40 °C for 43 h. The reaction mixture was then cooled to 0 °C and the sidearm was charged with 1 N HCl (5 mL). Opening the Teflon® screw cap allowed a rapid quench of the reaction mixture. The resulting solution was

extracted with CH_2Cl_2 (3 x 20 mL). The combined organic layers were dried over Na_2SO_4, filtered, and concentrated. ^{1}H NMR ratios for two trials indicated starting material product ratios of 13:1 and 12:1. Chromatography on SiO_2 with 20% EtOAc/hexanes allowed isolation of the starting material **2** (68.1 mg, 0.34 mmol, 80%) in accord with the ^{1}H NMR measurements and product in 91% ee. Assay procedure for enantiomeric excess of **3**: Chiralpak AD, 1.0 mL/min, 10% *i*-PrOH/hexanes, $t_R(R)$ = 11.2 min, $t_R(S)$ = 18.2 min.

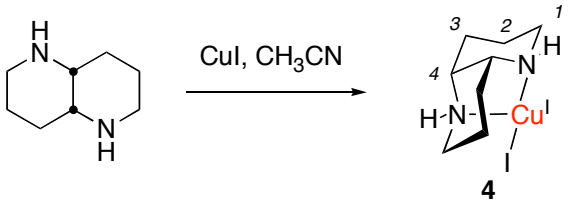

4

Preparation of 4. CH_3CN was degassed in a Schlenk tube by the freeze-pump-thaw method (3 cycles). In the glove box, a 1 mL volumetric flask was charged with 1,5-diaza-*cis*-decalin (5.7 mg, 0.041 mmol) and CuI (7.7 mg, 0.041 mmol), diluted with CH_3CN, and shaken for 1 h at room temperature to afford a clear-colorless, and homogeneous solution of **4** (0.041 M). The resulting solution was cooled to –20° C to afford colorless crystals of **4** suitable for crystallographic analysis (see end of Supporting Information for structure data tables). Crystalline complex **4** is stable indefinitely at room temperature in an inert atmosphere and undergoes surface oxidation very slowly in the presence of air. Solutions of **4** rapidly undergo oxidation when exposed to even trace amounts of atmosphere yielding pink to black solutions. ^{1}H NMR (500 MHz, CD_3CN) δ 3.17 (ddd, J = 1.5, 2.2, 11.7 Hz, 2H, *1e*), 2.80 (m, 2H, *4*), 2.69 (ddd, J = 1.5, 2.9, 12.4 Hz, 2H, *1a*), 2.22 (ddddd, J = 4.7, 4.7, 13.3, 13.3, 13.3 Hz, 2H, *2a*), 2.08 (s, 2H, *N-H*), 1.70 (m, 2H, *3a*), 1.64 (dddd, J = 4.8, 4.8, 13.5, 13.5, 2H, *3e*), 1.55 (m, 2H, *2e*); ^{13}C NMR (500 MHz, CD_3CN) δ 56.8, 49.7, 29.9, 23.0; IR (KBr pellet) 3458, 3248, 2932, 2833.

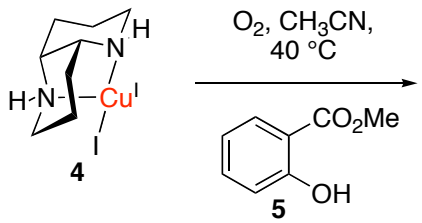

4 **5**

Oxidation of 4 in the Presence of Unreactive Phenol 5 (Figure S1). A solution of **5** in CH_3CN (5.0 mL, 239 μmol, 47.8 mM) was added to a reaction tube, attached to the O_2-uptake apparatus, evacuated, and backfilled with O_2 three times to 888 Torr, and thermally equilibrated at 40 °C. The reaction tube was charged with a solution of **4** in CH_3CN (3.0 mL, 90 μmol, 12 mM). Approximately 22.0 μmol of O_2 was absorbed corresponding to a 4:1 (**4**:O_2) stoichiometry of reaction.

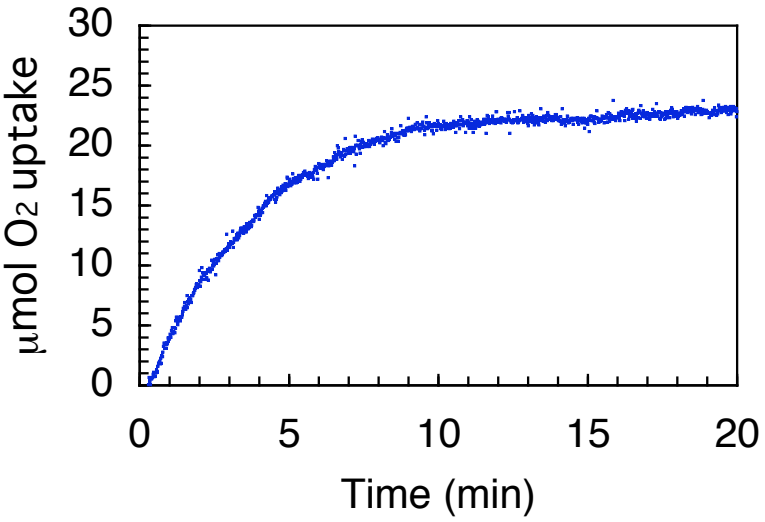

Figure S1. Dioxygen uptake for the oxidation of **4** in the presence of phenol **5**.

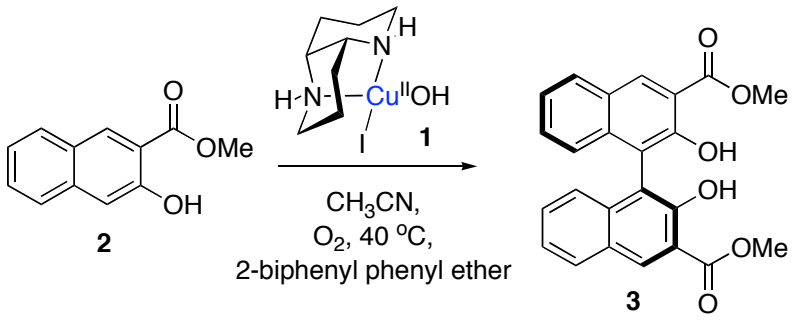

Discovery of the Initial Product Burst with 1 (Figure 1A, main text). A stock solution of **4** (0.01 M) in CH_3CN was prepared in an inert atmosphere glove box. A stock solution of **2** (0.12 M) combined with 4-biphenyl phenyl ether (0.029 M) in CH_3CN was prepared. A test tube was charged with 1.8 mL (0.217 mmol **2**, 0.053 mmol 4-biphenyl phenyl ether) of this stock solution, purged with dioxygen, and equilibrated to 40° C. The colorless copper(I) stock solution was removed from the glove box and sparged with dioxygen to afford a black solution of **1**. An aliquot of the resultant solution of **1** (0.5 mL,

0.005 mmol) was added and the resulting solution was stirred under atmospheric oxygen. Samples (100 μL) were taken over the course of one hour. Each sample was immediately quenched in 1 N HCl (0.5 mL), diluted with CH_2Cl_2, transferred to a vial and the subsequent analysis was performed by GC (Agilent 6850): t_R(**1**) = 1.14 min, t_R(4-biphenyl phenyl ether) = 4.8 min, t_R(**3**) = 20.4 min, *cf* = 1.18.

Table S1. Product formation with Cu(II) catalyst **1** (Figure 1A, main text).

time (min)	[**3**] (mM)	time (min)	[**3**] (mM)	time (min)	[**3**] (mM)
0.43	0.14	6.30	0.53	27.50	1.27
0.80	0.18	7.63	0.58	31.75	1.41
1.27	0.24	8.87	0.64	41.28	1.69
2.07	0.30	10.27	0.70	48.92	1.97
3.03	0.37	12.72	0.79	56.42	2.16
4.15	0.44	16.08	0.89	63.23	2.30
5.25	0.47	20.27	1.04		

Correlation of O_2 Uptake to Product Formation and Substrate Consumption (Figure 1B, main text). Five reaction tubes were charged with a stock solution (4 mL) of **2** (0.226 M, 904 μmol) combined with 4-biphenyl phenyl ether (0.063 M, 252 μmol) in MeCN. The tubes were sealed, charged with O_2 (840 Torr), and thermally equilibrated to 40° C. Each tube was then charged with **4** (2 mL, 30 mM, 60 μmol) to initiate the reaction. One tube was quenched with 1 N HCl (5 mL) at each of the times indicated in Table S2. The amounts of **2** and **3** were determined independently by GC (Shimadzu): t_R(**2**) = 4.1 min (*cf* = 0.586), t_R(4-biphenyl phenyl ether) = 12.9 min, t_R(**3**) = 24.5 min (*cf* = 0.663).

Table S2. Conversion analysis between O_2, **2**, and **3** (Figure 1B, main text).

tube	time (min)	Δ μmol **1**	(Δ μmol **1**)/4	Δ μmol **3**	(Δ μmol **3**)/2	Δ μmol O_2
1	1.70	44.1	11.0	3.10	1.50	11.00
2	3.90	60.6	15.1	8.50	4.30	13.80
3	9.70	107.3	26.8	29.0	14.5	29.33
4	20.0	159.5	39.9	59.8	29.9	44.18
5	29.9	215.5	53.9	92.1	46.1	56.73

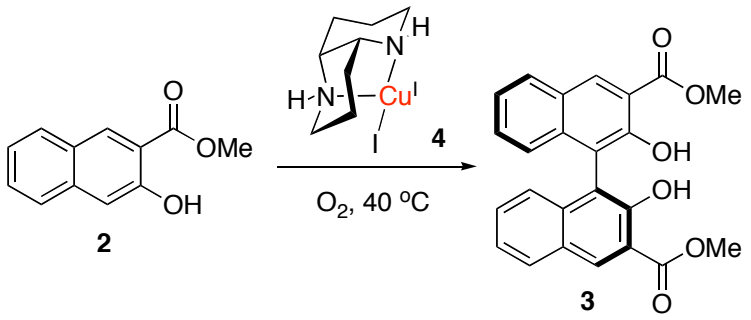

Stoichiometry of Dioxygen Uptake vs. Consumption of 2 (Figure S2). A stock solution of **4** (0.03 M) in CH_3CN was prepared in an inert atmosphere glove box. An oxygen uptake reaction tube was charged with stock solution of **2** (5 mL, 0.28 M, 1400 μmol), purged with dioxygen, and equilibrated to 40° C. Copper(I) complex **4**, was removed from the glove box (3 mL, 0.032 M, 96 μmol) and added to initiate the reaction. Consumption of 303 μmol of O_2 was observed (see Figure S2), after which the reaction was quenched with 1 N HCl (8 mL), extracted with CH_2Cl_2, washed with brine (5 mL), dried (Na_2SO_4), and concentrated *in vacuo*. Chromatography (10-20% EtOAc/hexanes) afforded **2** (42.9 mg, 212 μmol, 15%) indicating that 1188 μmol (283.1 mg, 85%) of **2** were consumed. The ratio of **2** consumed to O_2 is 3.9 which is consistent with:

1) All four oxidizing equivalents of O_2 being used in the OBC.
2) Four equivalents of substrate oxidized per equivalent of O_2 consumed.
3) Two equivalents of product formed per equivalent of O_2 consumed.

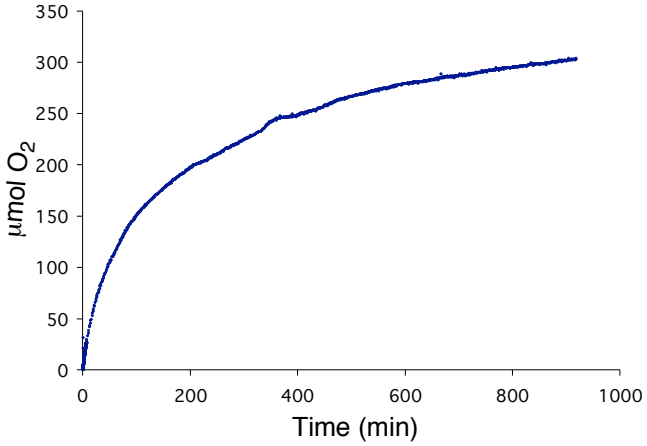

Figure S2. Dioxygen uptake for the oxidative biaryl coupling of **2**.

General Procedure for Gas-Uptake Rate Measurements. A typical procedure was conducted as follows for the catalyst dependence studies. A volumetric flask (10 mL) was taken into the glove box, charged with (*S*,*S*)-diaza-*cis*-decalin (49.3 mg, 352 μmol) and CuI (72.3 mg, 380 μmol), and diluted with degassed CH_3CN. The resulting mixture was shaken (1 h) to afford a clear, colorless, homogeneous solution of **4** (0.035 M). A separate volumetric flask (25 mL) was charged with **2** (1.21 g, 5.98 mmol) and diluted with CH_3CN. Each reaction tube (maximum of 6 total) was charged with a stir bar, the stock solution of **2** (3.5 mL, 0.24 M), and the required make-up volume of CH_3CN (0.5 – 3.2 mL). Each tube, with a known calibrated volume (solution plus headspace) was attached to the apparatus. The pressure within the sealed tube was measured with a pressure transducer. The reaction tubes were evacuated to 300 Torr and refilled with oxygen to 900 Torr, and this cycle was repeated 3 times. The pressure for each tube was established at 838 Torr and each flask was heated to 40 °C. Meanwhile the solution of **4** was taken up in a syringe (10 mL), the needle was plugged with a rubber septum, and removed from the glove box. When in the apparatus the pressure stabilized (849 Torr), **4** (0.3 – 3 mL) was added via syringe through a septum to provide a total reaction volume of 7.0 mL. Dioxygen uptake was monitored and the data was collected using custom software written within LabVIEW (National Instruments).

Steady-State Rate Extrapolation. The OBC reaction time-course reveals an unusual two-phase profile for the amount of O_2 consumed. There is an apparent burst in dioxygen uptake followed by a steady state (Figure S3). A plot of log μmols O_2 against time exhibits two first-order regimes (Figure S4) with a point of inflection at 2.2 minutes. Extrapolation of the rate from Figure S3 at the time of the point of inflection in Figure S4 is used to estimate the initial rate of the steady state.

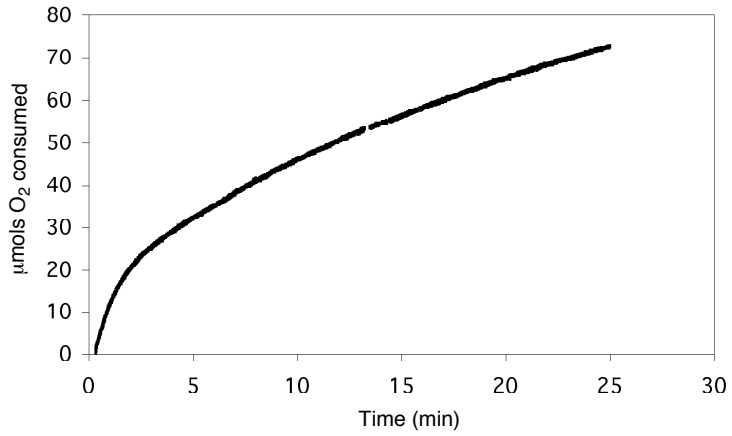

Figure S3. Kinetic time course for the OBC of **2** (0.12 M) with **4** (0.013 M). Conditions pO_2 = 849 torr, MeCN, 40 °C.

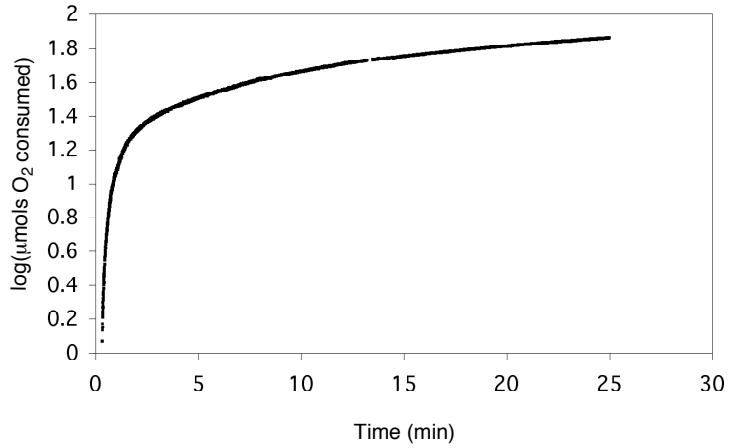

Figure S4. Log(μmol O_2 consumed) vs. time. Plot was generated using the primary data from Figure S3.

Steady-State Rate Dependence on [4].

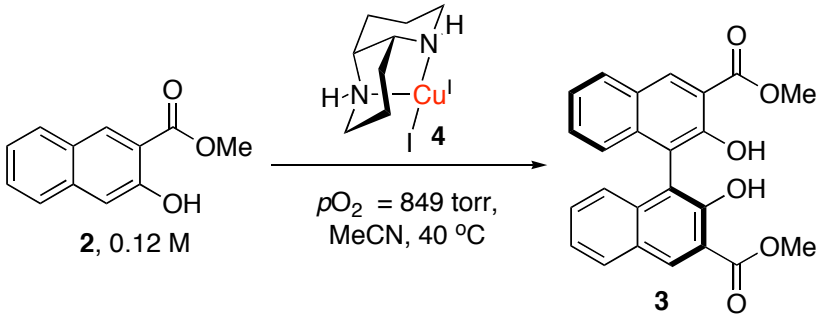

Table S3. Steady-state rate dependence on [**4**].

[**5**] (M)	rate (torr/min)	[**5**] (M)	rate (torr/min)
0.0015	0.066	0.0101	1.240
0.0040	0.469	0.0126	1.735
0.0060	0.713	0.0151	2.007

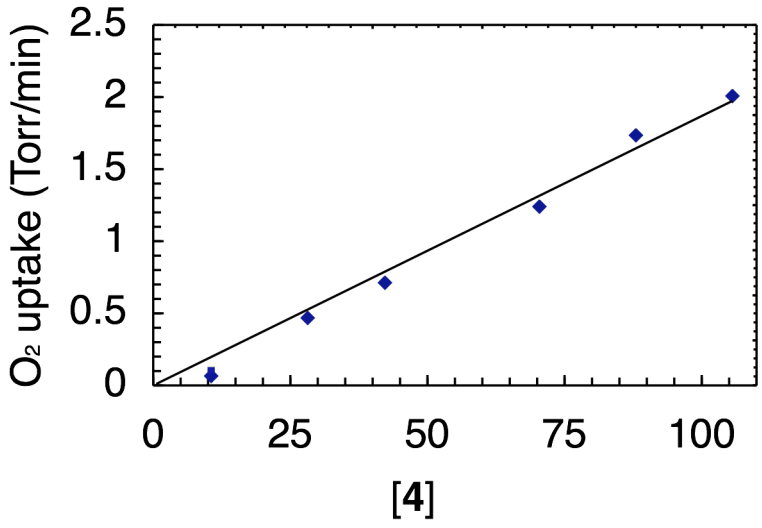

Figure S5. Steady-state rate dependence on [**4**].

Steady-State Rate Dependence on pO_2.

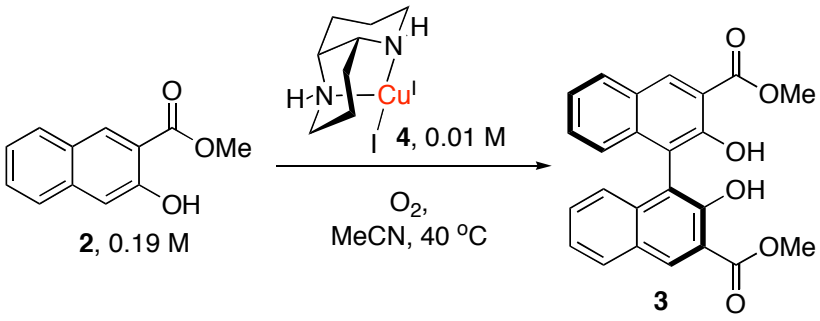

Table S4. Steady-state rate dependence on pO_2.

pO_2 (torr)	rate (torr/min)	pO_2 (torr)	rate (torr/min)
242	0.357	564	0.907
398	0.564	697	1.047

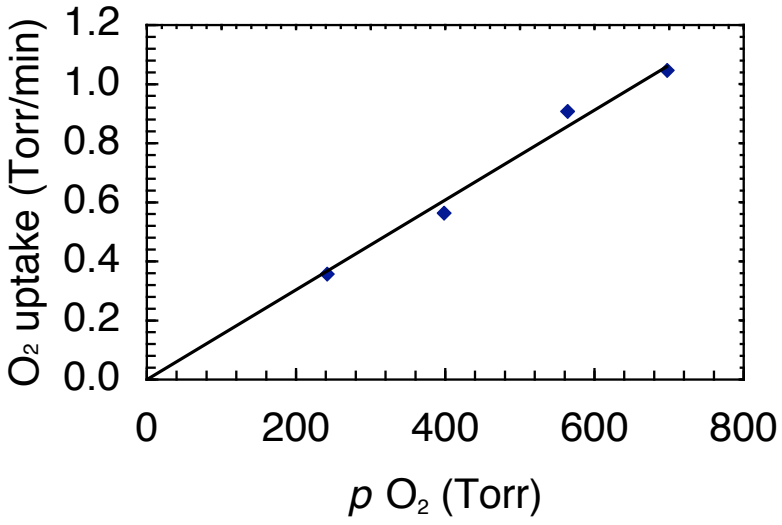

Figure S6. Steady-state rate dependence on pO_2.

Steady-State Rate Dependence on [2].

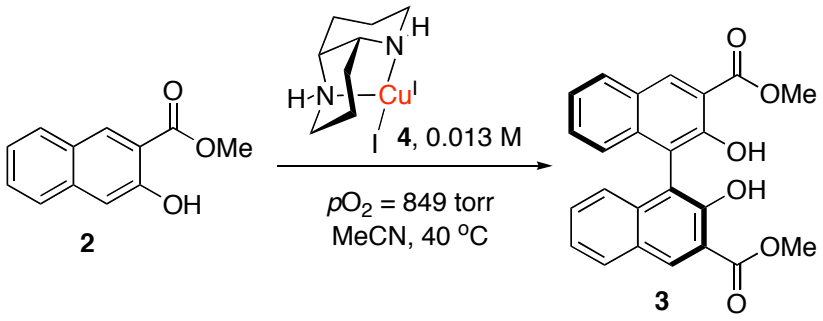

Table S5. Steady-state rate dependence on [**2**].

[**2**] (M)	rate (torr/min)	[**2**] (M)	rate (torr/min)
0.023	0.724	0.098	1.611
0.034	1.181	0.131	1.652
0.049	1.275		

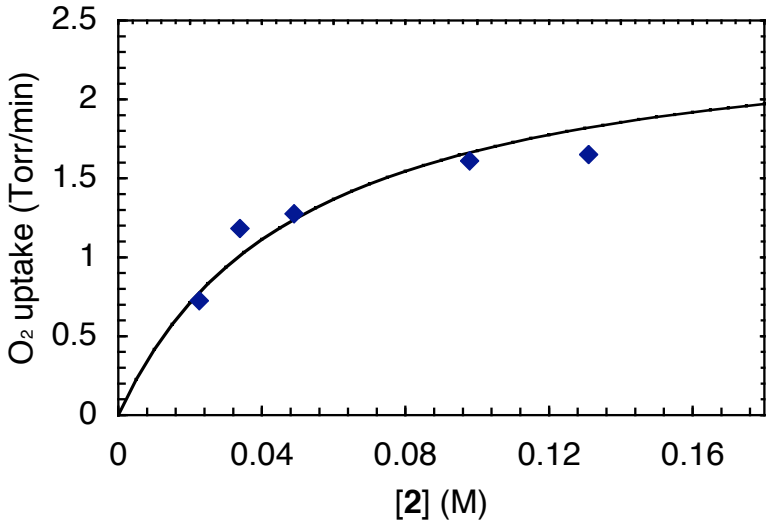

Figure S7. Steady-state rate dependence on [**2**].

Single Turnover under O_2 with Low Concentration of 4 - Isolation of ortho-Quinone Species: With high concentrations of **4** (i.e., stoichiometric) in the presence of O_2 and substrate **2**, formation of the oxidase steady state catalyst (**7**) occurs to some extent during the initial burst phase (oxidation of **4**) giving rise to OBC and formation of product **3**. To allow isolation of the putative cofactor $NapH^{OX}$, experiments were conducted with low concentrations of **4** and an excess of substrate **2**. These reactions were halted within the approximate window (5 min) of the burst phase (see Figure 1B, main text) to optimized formation of $NapH^{OX}$.

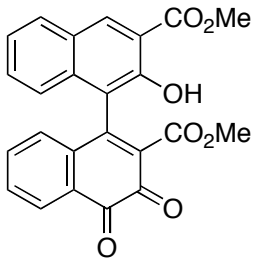

10

***ortho*-Quinone Dimer (10): Oxidation of Substrate 2 with 4.** A stock solution of CuI (135.3 mg, 0.710 mmol) and (*R*, *R*)-diaza-*cis*-decalin (99.0 mg, 0.707 mmol) in degassed CH_3CN (24 mL) was prepared in a three-neck round bottom flask. Substrate **2** (5.99 g, 29.62 mmol) was dissolved in CH_3CN (100 mL), sparged with O_2 and thermally equilibrated at 40 °C for 20 min. The solution of **4** was transferred via syringe and added in one portion to the solution of **2**. An immediate color change from yellow to dark green was observed. The resulting solution was stirred for 5 min and quenched with 1 N HCl (125 mL). The resulting orange mixture was extracted with CH_2Cl_2 (2 x 250 mL) and washed with brine (1 x 200 mL) and concentrated to give a dark brown solid. The resulting solid was diluted with CH_2Cl_2 however some colored solid material remained. Chromatography (10% EtOAc/hexanes) afforded **2** (5.925 g, 29.30 mmol; 0.32 mmol **2** consumed) and an inseparable mixture of trace **3** (< 2 mg) and oxidized **2** (32.3 mg). Chromatography (20% MeOH/CH_2Cl_2) of the resulting material again gave an inseparable mixture of colored products (9 mg). Preparative TLC (2.5% MeOH/CH_2Cl_2) afforded compound **OQD** (3 mg, 7.2 μmol) as an orange resin: IR (thin film) 3215, 2957, 2926, 1737, 1675; ^{1}H NMR (500 MHz, $CDCl_3$) δ 10.80 (s, 1H), 8.67 (s, 1H), 8.25 (m, 1H), 7.90 (m, 1H), 7.57 (m, 1H), 7.54 – 7.51 (m, 2H), 7.46 – 7.40 (m, 2H), 6.85 (m, 1H), 4.06 (s, 3H), 3.37 (s, 3H); ^{13}C NMR (500 MHz, $CDCl_3$) δ 171.0, 164.0, 153.2, 150.9, 136.1, 135.2, 134.8, 134.6, 134.5, 131.9, 131.1, 130.7 (2C), 130.6, 130.1(2C), 129.9, 129.1,

126.9, 124.9, 124.2, 114.0, 53.2, 52.4; HRMS (ES^+) calcd for $C_{24}H_{16}O_7Na$ (MNa^+) 439.0794, found 439.0777.

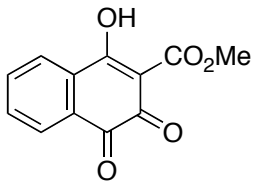

9

***ortho*-Quinone (9): Oxidation of Substrate 2 with 4.** Performed analogously to the procedure resulting in **10**. Crystals were isolated from a reaction mixture in 20% EtOAc/hexanes. IR (thin film) 3255, 3130, 2926, 2856, 1602; ^{1}H NMR (500 MHz, DMSO-d_6) δ 10.03 (brs, 1H), 9.41 (brs, 1H), 8.33 - 8.31 (m, 1H), 8.01 – 8.00 (m, 1H), 7.90 (t, 1H), 7.78 (m, 1H), 3.74 (s, 3H); ^{13}C NMR (500 MHz, DMSO-d_6) δ 180.7, 169.1, 160.7, 134.8, 132.9, 131.6, 130.0, 127.8, 125.3, 100.1, 51.3. See below from X-ray structural characterization.

X-Ray Structure Determination of 4. Compound **4**, $C_8H_{16}N_2ICu$, crystallizes in the orthorhombic space group $C222_1$ (systematic absences hkl: h+k = odd, 00l: l = odd) with a = 8.998(2) Å, b = 12.980(2) Å, c = 9.804(2) Å, V = 1145.0(3) $Å^3$, Z = 4 and d_{calc} = 1.918 g/cm^3. X-ray intensity data were collected on a Rigaku Mercury CCD area detector employing graphite-monochromated Mo-K_α radiation (λ = 0.71073 Å) at a temperature of 143 K. Preliminary indexing was performed from a series of twelve 0.5° rotation images with exposures of 30 seconds. A total of 440 rotation images were collected with a crystal to detector distance of 35 mm, a 2θ swing angle of –10°, rotation widths of 0.5° and exposures of 10 seconds: scan no. 1 was a ϕ-scan from –90° to 90° at ω = 0° and χ = 0°; scan no. 2 was an ω-scan from –20° to 20° at χ = –90° and ϕ = 0°. Rotation images were processed using CrystalClear[4], producing a listing of unaveraged F^2 and $\sigma(F^2)$ values which were then passed to the CrystalStructure[5] program package for further processing and structure solution on a Dell Pentium III computer. A total of 3284 reflections were measured over the ranges $5.5 \le 2\theta \le 50.0$ °, $-9 \le h \le 10$, $-15 \le k \le 12$, $-11 \le l \le 10$ yielding 995 unique reflections (R_{int} = 0.0270). The intensity data were corrected for Lorentz and polarization effects and for absorption using REQAB[6] (minimum and maximum transmission 0.701, 1.000).

The structure was solved by direct methods (SIR97[7]). The molecule lies on a crystallographic 2-fold axis parallel to ***a*** (at x, 1/2, 1/2); the Cu-I bond is conincident with the 2-fold axis. Refinement was by full-matrix least squares based on F^2 using SHELXL-97[8]. All reflections were used during refinement (F^2 's that were experimentally negative were replaced by $F^2 = 0$). The weighting scheme used was $w=1/[\sigma^2(F_o^2)+ 0.0476P^2 + 0.2870P]$ where $P = (F_o^2 + 2F_c^2)/3$. Non-hydrogen atoms were refined anisotropically and hydrogen atoms were refined using a "riding" model. Refinement converged to R_1=0.0296 and wR_2=0.0765 for 911 reflections for which $F > 4\sigma(F)$ and R_1=0.0331, wR_2=0.0786 and GOF = 1.098 for all 995 unique, non-zero reflections and 57 variables[9]. The maximum Δ/σ in the final cycle of least squares was 0.000 and the two most prominent peaks in the final difference Fourier were +1.438 and -0.980 $e/Å^3$.

Table S6 lists cell information, data collection parameters, and refinement data. Final positional and equivalent isotropic thermal parameters are given in Table S7. Anisotropic thermal parameters are in Table S8. Tables S9 and S10 list bond distances and bond angles. Figure S8 is an ORTEP[10] representation of the molecule with 30% probability thermal ellipsoids displayed.

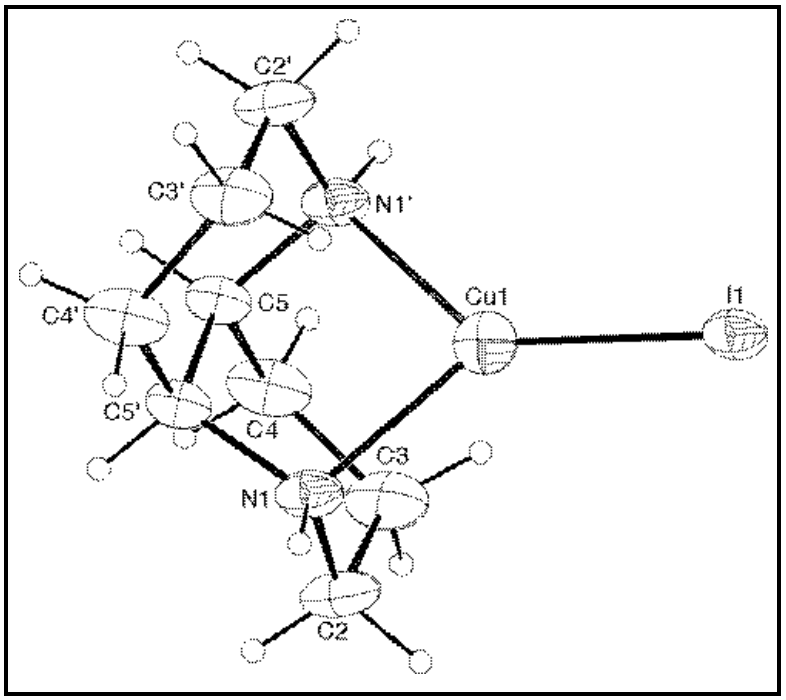

Figure S8. ORTEP drawing of **4** with 30% probability thermal ellipsoids.

Table S6. Summary of structure determination for compound **4**.

Formula:	$CuC_8H_{16}N_2I$
Formula weight:	330.67
Crystal class:	orthorhombic
Space group:	$C222_1$ (#20)
Z	4
Cell constants:	
a	8.998(2)Å
b	12.980(2)Å
c	9.804(2)Å
V	1145.0(3)Å^3
μ	45.59 cm^{-1}
crystal size, mm	0.28 x 0.16 x 0.12
D_{calc}	1.918 g/cm^3
F(000)	640
Radiation:	Mo-K_α (λ = 0.71073Å)
2θ range	5.5 – 50.0 °
hkl collected:	$-9 \le h \le 10$; $-15 \le k \le 12$; $-11 \le l \le 10$
No. reflections measured:	3284
No. unique reflections:	995 (R_{int}=0.0270)
No. observed reflections	911 (F>4σ)
No. reflections used in refinement	995
No. parameters	57
R indices (F>4σ)	R_1=0.0296
	wR_2=0.0765
R indices (all data)	R_1=0.0331
	wR_2=0.0786
GOF:	1.098
Final Difference Peaks, e/Å^3	+1.438, -0.980

Table S7. Refined positional parameters for compound **4**.

Atom	x	y	z	U_{eq}, Å^2
Cu1	0.48481(8)	0.5000	0.5000	0.0526(3)
I1	0.75222(4)	0.5000	0.5000	0.0476(2)
N1	0.3121(6)	0.4555(3)	0.6310(4)	0.0461(11)
H1	0.3303	0.4741	0.7190	0.061
C2	0.2960(10)	0.3428(4)	0.6159(6)	0.062(2)
H2a	0.2033	0.3202	0.6567	0.082
H2b	0.3772	0.3079	0.6618	0.082
C3	0.2976(9)	0.3165(3)	0.4634(5)	0.063(2)
H3a	0.3942	0.3329	0.4252	0.084
H3b	0.2803	0.2433	0.4513	0.084
C4	0.1785(8)	0.3769(4)	0.3893(6)	0.061(2)
H4a	0.0820	0.3485	0.4123	0.081
H4b	0.1926	0.3688	0.2918	0.081
C5	0.1792(6)	0.4929(6)	0.4241(5)	0.0448(11)
H5	0.0901	0.5252	0.3858	0.060

$U_{eq}=1/3[U_{11}(aa^*)^2+U_{22}(bb^*)^2+U_{33}(cc^*)^2+2U_{12}aa^*bb^*cos\gamma+2U_{13}aa^*cc^*cos\beta+2U_{23}bb^*cc^*cos\alpha]$

Table S8. Refined thermal parameters (U's) for compound **4**.

Atom	U_{11}	U_{22}	U_{33}	U_{23}	U_{13}	U_{12}
Cu1	0.0615(5)	0.0450(4)	0.0512(5)	-0.0091(6)	0.000	0.000
I1	0.0634(3)	0.0515(3)	0.0278(3)	0.0028(3)	0.000	0.000
N1	0.074(3)	0.039(2)	0.026(2)	-0.001(2)	0.000(2)	0.004(2)
C2	0.102(5)	0.038(3)	0.045(3)	0.011(2)	-0.004(4)	0.007(4)
C3	0.106(4)	0.030(2)	0.054(4)	-0.007(2)	0.006(4)	-0.004(3)
C4	0.098(5)	0.043(3)	0.042(3)	-0.007(3)	-0.003(3)	-0.024(3)
C5	0.061(3)	0.040(2)	0.034(2)	0.002(3)	0.000(2)	-0.010(5)

The form of the anisotropic displacement parameter is:

$\exp[-2\pi^2(a^{*2}U_{11}h^2+b^{*2}U_{22}k^2+c^{*2}U_{33}l^2+ 2b^*c^*U_{23}kl+2a^*c^*U_{13}hl+2a^*b^*U_{12}hk)]$.

Table S9. Bond distances in compound **4** (Å).

Cu1-N1’	2.097(5)	Cu1-N1	2.097(5)	Cu1-I1	2.4060(9)
N1-C5’	1.473(7)	N1-C2	1.478(6)	C2-C3	1.534(8)
C3-C4	1.513(9)	C4-C5	1.544(8)	C5-N1’	1.473(7)
C5-C5’	1.499(9)				

Table S10. Bond angles in compound **4** (deg).

N1’-Cu1-N1	84.4(2)	N1’-Cu1-I1	137.81(12)	N1-Cu1-I1	137.81(12)
C5’-N1-C2	109.5(6)	C5’-N1-Cu1	104.6(3)	C2-N1-Cu1	106.5(4)
N1-C2-C3	108.5(4)	C4-C3-C2	110.3(6)	C3-C4-C5	113.3(5)
N1’-C5-C5’	108.0(4)	N1’-C5-C4	111.4(5)	C5’-C5-C4	109.8(7)

X-Ray Structure Determination of 9. Compound **9**, $C_{25}H_{18}O_{10}Cl_2$, crystallizes in the triclinic space group $P\bar{1}$ with a=7.1311(4)Å, b=12.5109(7)Å, c=13.6583(8)Å, α=84.172(3)°, β=83.812(3)°, γ=79.439(3)°, V=1186.75(12)Å^3, Z=2 and d_{calc}=1.537 g/cm^3. X-ray intensity data were collected on a Rigaku Mercury CCD area detector employing graphite-monochromated Mo-K_α radiation (λ=0.71069 Å) at a temperature of 143 K. Preliminary indexing was performed from a series of twelve 0.5° rotation images with exposures of 60 seconds. A total of 708 rotation images were collected with a crystal to detector distance of 36 mm, a 2θ swing angle of -10°, rotation widths of 0.5° and exposures of 30 seconds: scan no. 1 was a ϕ-scan from 315° to 525° at ω = 10° and χ = 20°; scan no. 2 was an ω-scan from -20° to 20° at χ = -90° and ϕ = 135°; scan no. 3 was an ω-scan from -20° to 4° at χ = -90° and ϕ = 315°; scan no. 4 was an ω-scan from -20° to 20° at χ = -90° and ϕ = 0°; scan no. 5 was an ω-scan from -20° to 20° at χ = -90° and ϕ = 225°. Rotation images were processed using CrystalClear,[4] producing a listing of unaveraged F^2 and σ(F^2) values which were then passed to the CrystalStructure[5] program package for further processing and structure solution on a Dell Pentium III computer. A total of 11133 reflections were measured over the ranges $5.84 \le 2\theta \le 50.68$ °, $-8 \le h \le 8$, $-15 \le k \le 15$, $-16 \le l \le 16$ yielding 4310 unique reflections (R_{int} = 0.0170). The intensity data were corrected for Lorentz and polarization effects and for absorption. using REQAB[6] (minimum and maximum transmission 0.835, 1.000).

The structure was solved by direct methods (SIR97[7]). Refinement was by full-matrix least squares based on F^2 using SHELXL-97.[8] All reflections were used during refinement (F^2 's that were experimentally negative were replaced by F^2 = 0). The weighting scheme used was $w=1/[\sigma^2(F_o^2)+ 0.0922P^2 + 1.1736P]$ where $P = (F_o^2 + 2F_c^2)/3$. Non-hydrogen atoms were refined anisotropically and hydrogen atoms were refined using a "riding" model. Refinement converged to R_1=0.0564 and wR_2=0.1585 for 3777 reflections for which $F > 4\sigma(F)$ and R_1=0.0618, wR_2=0.1645 and GOF = 1.061 for all 4310 unique, non-zero reflections and 339 variables.[9] The maximum Δ/σ in the final cycle of least squares was 0.000 and the two most prominent peaks in the final difference Fourier were +0.782 and -0.625 e/Å^3.

Table S11 lists cell information, data collection parameters, and refinement data. Final positional and equivalent isotropic thermal parameters are given in Table S12. Anisotropic thermal parameters are in Table S13. Tables S14 and S15 list bond distances and bond angles. Figures S9 and S10 are ORTEP[10] representations of the molecule with 30% probability thermal ellipsoids displayed.

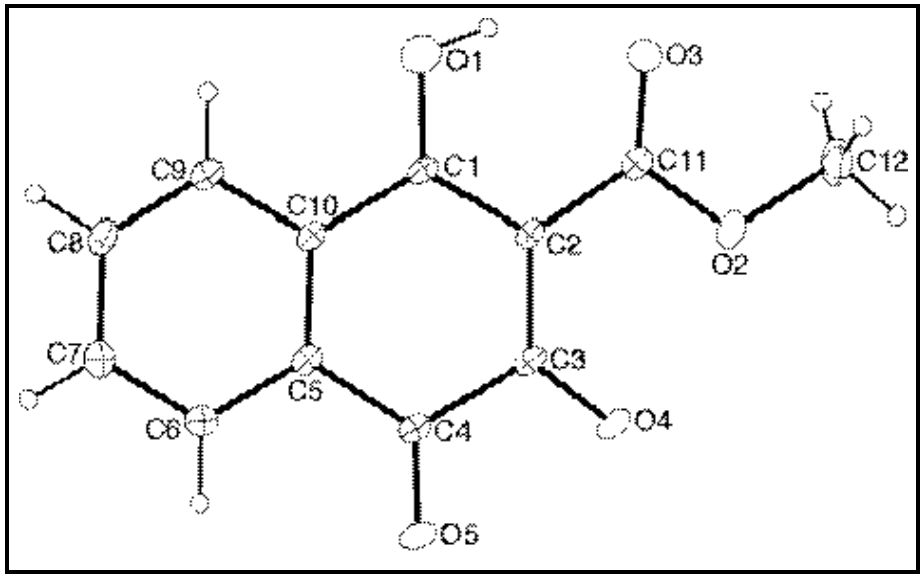

Figure S9. ORTEP drawing of molecule no. 1 of the asymmetric unit with 30% probability thermal ellipsoids.

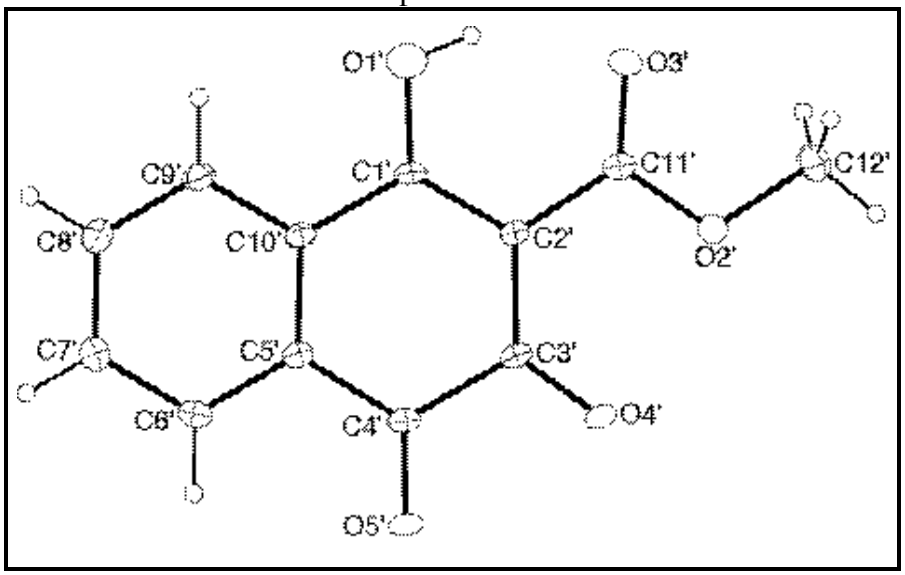

Figure S10. ORTEP drawing of molecule no. 2 of the asymmetric unit with 30% probability thermal ellipsoids.

Table S11. Summary of Structure Determination of Compound **9**.

Formula:	$C_{25}H_{18}O_{10}Cl_2$
Formula weight:	549.29
Crystal class:	triclinic
Space group:	$P\bar{1}$ (#2)
Z	2
Cell constants:	
a	7.1311(4)Å
b	12.5109(7)Å
c	13.6583(8)Å
α	84.172(3)°
β	83.812(3)°
γ	79.439(3)°
V	1186.75(12)Å^3
μ	3.34 cm^{-1}
crystal size, mm	0.32 x 0.30 x 0.15
D_{calc}	1.537 g/cm^3
F(000)	564
Radiation:	Mo-K_α (λ=0.71069Å)
2θ range	5.84 – 50.68 °
hkl collected:	-8≤ h ≤8; -15≤ k ≤15; -16≤ l ≤16
No. reflections measured:	11133
No. unique reflections:	4310 (R_{int}=0.0170)
No. observed reflections	3777 (F>4σ)
No. reflections used in refinement	4310
No. parameters	339
R indices (F>4σ)	R_1=0.0564
	wR_2=0.1585
R indices (all data)	R_1=0.0618
	wR_2=0.1645
GOF:	1.061
Final Difference Peaks, e/Å^3	+0.782, -0.625

Table S12. Refined Positional Parameters for Compound **9**.

Atom	x	y	z	U_{eq}, Å^2
C1	0.5932(3)	0.4858(2)	0.6565(2)	0.0180(5)
C2	0.6879(3)	0.4214(2)	0.5794(2)	0.0188(5)
C3	0.7755(3)	0.4723(2)	0.4922(2)	0.0214(5)
C4	0.7579(3)	0.5970(2)	0.4815(2)	0.0212(5)
C5	0.6709(3)	0.6587(2)	0.5660(2)	0.0205(5)
C6	0.6727(3)	0.7707(2)	0.5604(2)	0.0262(5)
H6	0.7311	0.8045	0.5045	0.035
C7	0.5879(4)	0.8311(2)	0.6376(2)	0.0287(5)
H7	0.5901	0.9055	0.6344	0.038
C8	0.4995(3)	0.7799(2)	0.7197(2)	0.0263(5)
H8	0.4390	0.8207	0.7710	0.035
C9	0.4998(3)	0.6689(2)	0.7265(2)	0.0232(5)
H9	0.4415	0.6358	0.7828	0.031
C10	0.5869(3)	0.6059(2)	0.6497(2)	0.0177(4)
C11	0.6952(3)	0.3021(2)	0.5923(2)	0.0223(5)
C12	0.7937(5)	0.1322(2)	0.5279(2)	0.0403(7)
H12a	0.8417	0.1020	0.5897	0.060
H12b	0.8752	0.0992	0.4746	0.060
H12c	0.6662	0.1181	0.5265	0.060
O1	0.5103(3)	0.4412(2)	0.73723(14)	0.0379(5)
H1	0.5269	0.3749	0.7349	0.057
O2	0.7906(3)	0.24787(14)	0.51750(13)	0.0334(4)
O3	0.6197(3)	0.25360(14)	0.66319(13)	0.0328(4)
O4	0.8658(3)	0.42543(14)	0.42203(12)	0.0339(4)
O5	0.8152(3)	0.64086(14)	0.40335(12)	0.0312(4)
C1'	0.9090(3)	0.5240(2)	0.8432(2)	0.0174(4)
C2'	0.8247(3)	0.4618(2)	0.9233(2)	0.0173(4)
C3'	0.7376(3)	0.5124(2)	1.0106(2)	0.0186(5)
C4'	0.7388(3)	0.6343(2)	1.0157(2)	0.0198(5)
C5'	0.8209(3)	0.6964(2)	0.9294(2)	0.0194(5)
C6'	0.8134(3)	0.8086(2)	0.9322(2)	0.0256(5)

H6'	0.7533	0.8434	0.9871	0.034
C7'	0.8952(4)	0.8675(2)	0.8534(2)	0.0284(5)
H7'	0.8907	0.9420	0.8550	0.038
C8'	0.9839(4)	0.8150(2)	0.7722(2)	0.0282(5)
H8'	1.0402	0.8546	0.7194	0.037
C9'	0.9903(3)	0.7038(2)	0.7682(2)	0.0235(5)
H9'	1.0504	0.6697	0.7129	0.031
C10'	0.9071(3)	0.6432(2)	0.8466(2)	0.0178(4)
C11'	0.8258(3)	0.3456(2)	0.9134(2)	0.0200(5)
C12'	0.7264(4)	0.1822(2)	0.9773(2)	0.0376(6)
H12a'	0.6678	0.1777	0.9181	0.056
H12b'	0.6532	0.1525	1.0332	0.056
H12c	0.8545	0.1415	0.9727	0.056
O1'	0.9915(3)	0.4794(2)	0.76271(13)	0.0371(5)
H1'	0.9844	0.4143	0.7680	0.056
O2'	0.7318(3)	0.29485(14)	0.98900(12)	0.0297(4)
O3'	0.9038(3)	0.29584(14)	0.84349(12)	0.0296(4)
O4'	0.6632(2)	0.46666(14)	1.08479(11)	0.0279(4)
O5'	0.6740(2)	0.67609(14)	1.09190(11)	0.0288(4)
C13	0.7185(4)	0.8633(2)	0.2364(2)	0.0338(6)
H13a	0.6452	0.8137	0.2761	0.045
H13b	0.8151	0.8206	0.1938	0.045
Cl1	0.8300(2)	0.93011(7)	0.31388(7)	0.0654(3)
Cl2	0.56590(13)	0.95729(6)	0.16393(6)	0.0559(3)

$U_{eq}=1/3[U_{11}(aa^*)^2+U_{22}(bb^*)^2+U_{33}(cc^*)^2+2U_{12}aa^*bb^*cos\gamma+2U_{13}aa^*cc^*cos\beta+2U_{23}bb^*cc^*cos\alpha]$

Table S13. Refined Thermal Parameters (U's) for Compound **9**.

Atom	U_{11}	U_{22}	U_{33}	U_{23}	U_{13}	U_{12}
C1	0.0162(10)	0.0261(12)	0.0116(10)	-0.0023(8)	-0.0004(8)	-0.0032(8)
C2	0.0195(10)	0.0218(11)	0.0146(10)	-0.0050(9)	0.0002(8)	-0.0017(9)
C3	0.0220(11)	0.0273(12)	0.0135(10)	-0.0037(9)	0.0013(8)	-0.0008(9)
C4	0.0209(11)	0.0262(12)	0.0159(10)	-0.0023(9)	0.0010(8)	-0.0034(9)
C5	0.0200(10)	0.0244(12)	0.0166(10)	-0.0039(9)	0.0000(8)	-0.0022(9)
C6	0.0309(12)	0.0253(12)	0.0217(11)	-0.0006(9)	0.0019(9)	-0.0066(10)
C7	0.0330(13)	0.0226(12)	0.0306(13)	-0.0060(10)	-0.0012(10)	-0.0036(10)
C8	0.0291(12)	0.0259(12)	0.0232(12)	-0.0098(9)	0.0013(9)	-0.0010(10)
C9	0.0230(11)	0.0273(12)	0.0181(11)	-0.0034(9)	0.0024(9)	-0.0033(9)
C10	0.0162(10)	0.0232(11)	0.0138(10)	-0.0048(8)	-0.0002(8)	-0.0028(8)
C11	0.0229(11)	0.0252(12)	0.0185(11)	-0.0045(9)	-0.0015(9)	-0.0020(9)
C12	0.058(2)	0.0246(13)	0.037(2)	-0.0108(11)	-0.0066(13)	0.0011(12)
O1	0.0430(11)	0.0385(11)	0.0318(10)	-0.0036(8)	0.0009(8)	-0.0078(9)
O2	0.0499(11)	0.0224(9)	0.0251(9)	-0.0086(7)	0.0058(8)	-0.0006(8)
O3	0.0440(10)	0.0240(9)	0.0286(9)	-0.0029(7)	0.0084(8)	-0.0078(8)
O4	0.0497(11)	0.0284(9)	0.0183(8)	-0.0063(7)	0.0143(8)	-0.0008(8)
O5	0.0422(10)	0.0315(10)	0.0176(8)	-0.0015(7)	0.0094(7)	-0.0076(8)
C1'	0.0144(10)	0.0248(11)	0.0125(10)	-0.0057(8)	-0.0008(8)	-0.0001(8)
C2'	0.0161(10)	0.0216(11)	0.0140(10)	-0.0031(8)	-0.0006(8)	-0.0024(8)
C3'	0.0167(10)	0.0254(12)	0.0135(10)	-0.0029(9)	0.0006(8)	-0.0033(9)
C4'	0.0188(10)	0.0241(12)	0.0156(10)	-0.0051(9)	0.0007(8)	-0.0006(9)
C5'	0.0192(10)	0.0227(11)	0.0157(10)	-0.0025(9)	-0.0007(8)	-0.0024(9)
C6'	0.0288(12)	0.0248(12)	0.0229(11)	-0.0082(9)	0.0009(9)	-0.0024(10)
C7'	0.0341(13)	0.0223(12)	0.0291(13)	-0.0023(10)	-0.0005(10)	-0.0068(10)
C8'	0.0321(12)	0.0278(13)	0.0244(12)	0.0009(10)	0.0010(10)	-0.0086(10)
C9'	0.0241(11)	0.0275(12)	0.0184(11)	-0.0036(9)	0.0033(8)	-0.0054(9)
C10'	0.0156(10)	0.0230(11)	0.0145(10)	-0.0028(8)	-0.0017(8)	-0.0020(8)
C11'	0.0175(10)	0.0252(12)	0.0173(10)	-0.0046(9)	-0.0013(8)	-0.0022(9)
C12'	0.049(2)	0.0267(14)	0.040(2)	-0.0092(11)	0.0066(12)	-0.0179(12)
O1'	0.0408(10)	0.0381(11)	0.0310(10)	-0.0068(8)	0.0004(8)	-0.0034(9)
O2'	0.0395(10)	0.0247(9)	0.0267(9)	-0.0075(7)	0.0090(7)	-0.0144(7)
O3'	0.0383(10)	0.0244(9)	0.0247(9)	-0.0089(7)	0.0075(7)	-0.0043(7)
O4'	0.0388(10)	0.0270(9)	0.0162(8)	-0.0041(7)	0.0101(7)	-0.0074(7)
O5'	0.0393(10)	0.0283(9)	0.0169(8)	-0.0083(7)	0.0083(7)	-0.0033(7)
C13	0.0373(14)	0.0234(13)	0.0399(14)	-0.0058(11)	0.0022(11)	-0.0047(10)
Cl1	0.0928(7)	0.0473(5)	0.0693(6)	0.0121(4)	-0.0439(5)	-0.0346(5)
Cl2	0.0776(6)	0.0304(4)	0.0627(5)	-0.0152(3)	-0.0330(4)	0.0044(4)

The form of the anisotropic displacement parameter is:
$\exp[-2\pi^2(a^{*2}U_{11}h^2+b^{*2}U_{22}k^2+c^{*2}U_{33}l^2+ 2b^*c^*U_{23}kl+2a^*c^*U_{13}hl+2a^*b^*U_{12}hk)]$.

Table S14. Bond Distances in Compound **9** (Å).

C1-O1	1.316(3)	C1-C2	1.426(3)	C1-C10	1.488(3)
C2-C3	1.430(3)	C2-C11	1.477(3)	C3-O4	1.232(3)
C3-C4	1.536(3)	C4-O5	1.215(3)	C4-C5	1.471(3)
C5-C10	1.396(3)	C5-C6	1.397(3)	C6-C7	1.381(3)
C7-C8	1.384(3)	C8-C9	1.382(3)	C9-C10	1.398(3)
C11-O3	1.218(3)	C11-O2	1.338(3)	C12-O2	1.436(3)
C1'-O1'	1.315(3)	C1'-C2'	1.422(3)	C1'-C10'	1.494(3)
C2'-C3'	1.434(3)	C2'-C11'	1.473(3)	C3'-O4'	1.231(3)
C3'-C4'	1.534(3)	C4'-O5'	1.221(3)	C4'-C5'	1.472(3)
C5'-C10'	1.398(3)	C5'-C6'	1.399(3)	C6'-C7'	1.379(3)
C7'-C8'	1.381(3)	C8'-C9'	1.390(3)	C9'-C10'	1.391(3)
C11'-O3'	1.220(3)	C11'-O2'	1.338(3)	C12'-O2'	1.442(3)
C13-Cl1	1.748(3)	C13-Cl2	1.754(3)		

Table S15. Bond Angles in Compound **9** (deg).

O1-C1-C2	121.4(2)	O1-C1-C10	117.3(2)	C2-C1-C10	121.4(2)
C1-C2-C3	120.1(2)	C1-C2-C11	118.7(2)	C3-C2-C11	121.2(2)
O4-C3-C2	126.2(2)	O4-C3-C4	115.0(2)	C2-C3-C4	118.8(2)
O5-C4-C5	122.6(2)	O5-C4-C3	118.6(2)	C5-C4-C3	118.7(2)
C10-C5-C6	121.0(2)	C10-C5-C4	120.2(2)	C6-C5-C4	118.9(2)
C7-C6-C5	120.1(2)	C6-C7-C8	119.3(2)	C9-C8-C7	120.9(2)
C8-C9-C10	120.7(2)	C5-C10-C9	118.0(2)	C5-C10-C1	120.4(2)
C9-C10-C1	121.6(2)	O3-C11-O2	120.4(2)	O3-C11-C2	124.9(2)
O2-C11-C2	114.7(2)	C11-O2-C12	115.2(2)	O1'-C1'-C2'	121.6(2)
O1'-C1'-C10'	117.1(2)	C2'-C1'-C10'	121.3(2)	C1'-C2'-C3'	120.3(2)
C1'-C2'-C11'	118.4(2)	C3'-C2'-C11'	121.2(2)	O4'-C3'-C2'	126.0(2)
O4'-C3'-C4'	115.3(2)	C2'-C3'-C4'	118.7(2)	O5'-C4'-C5'	122.2(2)
O5'-C4'-C3'	118.7(2)	C5'-C4'-C3'	119.1(2)	C10'-C5'-C6'	120.7(2)
C10'-C5'-C4'	120.1(2)	C6'-C5'-C4'	119.1(2)	C7'-C6'-C5'	120.0(2)
C6'-C7'-C8'	119.6(2)	C7'-C8'-C9'	120.9(2)	C8'-C9'-C10'	120.3(2)
C9'-C10'-C5'	118.5(2)	C9'-C10'-C1'	121.2(2)	C5'-C10'-C1'	120.3(2)
O3'-C11'-O2'	120.3(2)	O3'-C11'-C2'	125.0(2)	O2'-C11'-C2'	114.7(2)
C11'-O2'-C12'	114.6(2)	Cl1-C13-Cl2	110.85(14)		

References.

(1) Li, X.; Schenkel, L. B.; Kozlowski, M. C. *Org. Lett.* **2000**, *2*, 975-978.

(2) Still, W. C.; Kahn, M.; Mitra, A. *J. Org. Chem.* **1978**, *43*, 2923-2925.

(3) (a) Steinhoff, B. A.; Guzei, I. A.; Stahl, S. S. *J. Am. Chem. Soc.* **2004**, *126*, 11268-11278. (b) Steinhoff, B. A.; Stahl, S. S. *Org. Lett.* **2002**, *4*, 4179-4181.

(4) CrystalClear: Rigaku Corporation, 1999.

(5) CrystalStructure: Crystal Structure Analysis Package, Rigaku Corp. Rigaku/MSC (2002).

(6) REQAB4: R.A. Jacobsen, (1994). Private Communication.

(7) SIR97: Altomare, A., M. Burla, M. Camalli, G. Cascarano, C. Giacovazzo, A. Guagliardi, A. Moliterni, G. Polidori & R. Spagna (1999). *J. Appl. Cryst.*, **32**, 115-119.

(8) SHELXL-97: Program for the Refinement of Crystal Structures, Sheldrick, G.M. (1997), University of Göttingen, Germany.

(9) $R_1 = \sum ||F_o| - |F_c|| / \sum |F_o|$
$wR_2 = \{ \sum w (F_o^2 - F_c^2)^2 / \sum w(F_o^2)^2 \}^{1/2}$
$GOF = \{ \sum w (F_o^2 - F_c^2)^2 / (n - p) \}^{1/2}$ where n = the number of reflections and p = the number of parameters refined.

(10) "ORTEP-II: A Fortran Thermal Ellipsoid Plot Program for Crystal Structure Illustrations". C. K. Johnson (1976) ORNL-5138.